



national accelerator laboratory

NAL-Pub-73/24-EXP
7200.037

UCLA-1074
(Submitted to Physics Letters B)

pp INTERACTIONS AT 303 GeV/c:
PRODUCTION ANGLE DISTRIBUTION

F. T. Dao, D. Gordon, J. Lach, E. Malamud, and J. Schivell
National Accelerator Laboratory
Batavia, Illinois 60510

and

T. Meyer, R. Poster, P. E. Schlein, and W. E. Slater
University of California at Los Angeles
Los Angeles, California 90024

May 1973



Some recent studies of multiparticle reactions at very high energy have focussed on the nature of correlations between produced particles by measuring their approximate rapidity.¹ In this letter we report on a measurement at 303 GeV/c of projected production angles and the approximate rapidity derived from them. These data yield information on correlations at the highest accelerator energy. The sample of film is from an exposure of the NAL 30-inch bubble chamber to protons at 303 GeV/c, and is the same film as that used in a measurement of total cross section and multiplicity, reported in an earlier letter.² We chose to measure the angles in one view only, in order to obtain high statistics rapidly, at the cost of more difficult interpretation of the results.

A fiducial volume cut and rejection of odd-prong events reduced the sample from the 2245 events in Ref. 2 to 1739 events. Of these, 104 were lost due to measuring and bookkeeping problems, leaving 1635 events for which we measured all tracks. We believe the bias introduced by these losses to be negligible. At least half of the unmeasurable events were due to overlapping events or tracks in the same frame. Furthermore, these events have a fairly normal multiplicity distribution. Therefore, we have assumed that their rejection biases our results very little.

Measurement of an event consisted of digitizing ten sets of coordinates on each track. A parabola was fitted to the coordinates, and the production angle was obtained from the

slope at the vertex. In the case of a track with large curvature, we dropped points from the far end of the track until a good fit to a parabola was obtained. A minimum of four points was kept.

The results are analyzed in terms of rapidity, although we cannot measure the true rapidity. If a particle is produced with energy E and longitudinal momentum $p_{||}$, then the true rapidity is $y = 1/2 \log_e [(E + p_{||})/(E - p_{||})]$. If the mass of the particle is m , and one makes the approximation $m \rightarrow 0$, then $y \rightarrow \eta$ where $\eta = -\log_e (\tan \theta/2)$, and θ is the production angle. We measure the projected production angle, θ_p , and define $\eta_p = -\log_e (\tan \theta_p/2)$, which we refer to as the "pseudo-rapidity".

We have examined the distributions in η_p for positive and negative tracks separately for three ranges of multiplicity. Figure 1 shows these distributions. Due to the small size of the chamber, we have some difficulty identifying the charge of fast particles. In Fig. 1 the cross-hatched histograms include particles from only those events in which the sum of the measured charges was +2, while the open histograms include the particles from all events. We estimate that the amount of positive-negative mixing remaining in the cross-hatched histograms is less than 2%.

Note that $\eta_p = 0$ corresponds to 90° in the laboratory and that $\eta_p = 7.6$ corresponds to $\theta_p = 1$ milliradian, which is the limit of our resolution. The effects of using projected angles are to shift the means of the distributions positive by approximately one unit of η and to broaden and skew them slightly. Tracks with $\eta_p < 0$ are shifted to more negative values by projection.

Due to the skewing and our limited statistics we would not be able to distinguish a flat top 1.5 to 2 units wide, as has been observed in ISR experiments^{3,4} and in our analysis of inclusive γ production at this energy.⁵

For the lower multiplicities there is a distinct difference between the positives and the negatives. The broadening in the distribution of positive particles indicates that protons appear preferentially farther from the center of the rapidity distribution. We observe a possible narrowing of the negative (predominantly π) distribution as a function of n_{ch} . In order to obtain a numerical measure of the effect, we have calculated σ , the standard deviation from the mean, for the three negative η_p distributions. Only the events in which the total charge balanced were used. We have chosen to neglect the tails with $\eta_p < 0$ because they are distorted toward the left by the projection of angles, and because they significantly increase σ for the low and middle n_{ch} bins. (The tails on the right are shifted the same way as the bulk of the data and so do not cause a similar effect.) The values of σ are 1.73 ± 0.04 , 1.61 ± 0.03 , and 1.47 ± 0.04 for $4 \leq n_{ch} \leq 8$, $10 \leq n_{ch} \leq 14$, and $16 \leq n_{ch} \leq 20$, respectively. Narrowing in the η_p distribution would be similar to that seen in an experiment at the ISR⁴ at $s = 950 \text{ GeV}^2$. An additional salient feature of the data on negative particles is the strong central peak near $\eta_p = 4$.

We have also studied the dispersion of rapidity in individual events. This quantity can give a measure of the clustering of produced particles. Following a suggestion of Berger, et al.,⁶ we define two dispersion quantities, δ^0 and δ^{\perp} , as follows.

Let

$$\bar{n}_p = \frac{1}{n_{ch}} \sum_{i=1}^{n_{ch}} n_{pi}, \quad (1)$$

where n_{ch} is the number of charged particles from an event.

Then δ^0 is defined by

$$\delta^0 = \left[\frac{1}{n_{ch}-1} \sum_{i=1}^{n_{ch}} (n_{pi} - \bar{n}_p)^2 \right]^{1/2} \quad (2)$$

Then we find the n_{pj} such that $|n_{pi} - \bar{n}_p|$ is the largest for $i = j$ and call particle j the "leading particle". We define the mean \bar{n}_p^{-1} for all the rest of the particles by

$$\bar{n}_p^{-1} = \frac{1}{n_{ch}-1} \sum_{i=1}^{n_{ch}} n_{pi} \quad (i=j \text{ excluded}) \quad (3)$$

and the dispersion for all particles except the leading one by

$$\delta^1 = \left[\frac{1}{n_{ch}-2} \sum_{i=1}^{n_{ch}} (n_{pi} - \bar{n}_p^{-1})^2 \right]^{1/2} \quad (i=j \text{ excluded}) \quad (4)$$

Figure 2 shows the distributions of δ^1 for separate values of the multiplicity, n_{ch} . The enhancement at low δ^1 for events with $n_{ch} = 4$ is consistent with the low missing-mass enhancement observed in the slow proton studies at this energy.⁷ Figure 3, parts (a) and (b), shows the mean values of δ^0 and of δ^1 plotted against multiplicity. The removal of the "leading particle" from δ has a pronounced effect, even up to high multiplicities. The mean dispersions $\bar{\delta^1}$ are remarkably constant over $6 \leq n_{ch} \leq 16$. Figure 3(c) shows w^1 , the standard deviation of δ^1 , as a function of n_{ch} .

Berger, Fox, and Krzywicki have studied the usefulness of

event dispersion for distinguishing between multiperipheral and nova-type models.⁶ Professor Fox has calculated $\overline{\delta^1}$ and w^1 as a function of n_{ch} at 300 GeV for three representative models:

1) single and double nova production, 2) multiperipheral production of clusters, and 3) multiperipheral production of π 's. The calculated values are given as the curves in Figs. 3(b) and 3(c). The calculations contain adjustable parameters and are meant only to show the general features of the predictions of the three types of model. In particular, a strong prediction of the multiperipheral type of model, (2) and (3), is an $n_{ch}^{-1/2}$ dependence for w^1 . In fact, the measured values of w^1 can be fitted with the function $w^1 = 1.22 n_{ch}^{-1/2}$ ($\chi^2 = 10$ for 10 degrees of freedom. This function is not drawn in).

One might expect multiparticle production to contain both diffraction excitation⁷ and independent pion emission. Then one would expect a model like (1) to make a large contribution at lower n_{ch} and a model like (2) or (3) to dominate at higher n_{ch} . It appears reasonable that combining calculations (1) and (2) in this way could yield a prediction for $\overline{\delta^1}$ vs. n_{ch} in reasonable agreement with the data. In the case of w^1 , however, obtaining agreement appears more difficult.

We gratefully acknowledge enlightening conversations with G. Fox, M. Jacob, and W. Frazer. We also acknowledge the exceptional efforts of the scanning staff. This work would not have been possible without the dedicated support of the operation staffs of the accelerator, the Neutrino Laboratory, the 30-inch Bubble Chamber, and the Film Analysis Facility.

REFERENCES

*Work supported by the U. S. National Science Foundation under Grant GP-33565.

¹For a recent review, see M. Jacob, Proc. XVI International Conference on High Energy Physics, V. 3, p. 373 (National Accelerator Laboratory, Batavia, Ill. 1972).

²F. T. Dao, et al., Phys. Rev. Letters 29, 1627 (1972).

³G. Barbiellini, et al., Phys. Letters 39B, 294 (1972), and M. Breidenbach, et al., Phys. Letters 39B, 654 (1972).

⁴M. Belletini, report to the XVI International Conference on High Energy Physics, op. cit., V. 1, p. 279.

⁵F. T. Dao, et al., "pp Interactions at 303 GeV/c: Inclusive Studies of γ , K_S^0 , and Λ^0 Production", NAL-Pub 73/21-EXP and UCLA-1071, (to be published).

⁶E. Berger, G. Fox, and A. Krzywicki, Ref. TH.1593-CERN (unpublished) (1972).

⁷F. T. Dao, et al., "pp Interactions at 303 GeV/c: Analysis of the Reaction $pp \rightarrow pX$ ", NAL-Pub 73/22-EXP and UCLA-1072, (to be published).

⁸Geoffrey Fox, private communication.

FIGURE CAPTIONS

Fig. 1. Semi-inclusive distributions of pseudo-rapidity in three ranges of charged multiplicity, n_{ch} . Negative and positive particles are shown separately. Open histograms: all events; hatched histograms: events with sum of charge = +2.

Fig. 2. Distributions of event dispersion, δ^1 (see text) for values of charged multiplicity from 4 to 14.

Fig. 3. Event dispersion as a function of charged multiplicity; (a) Mean values of δ^0 . (b) Mean values of δ^1 . (c) w^1 , the standard deviation of δ^1 . The curves are calculations for three models (see text).

303 GeV/c PP
NAL-UCLA

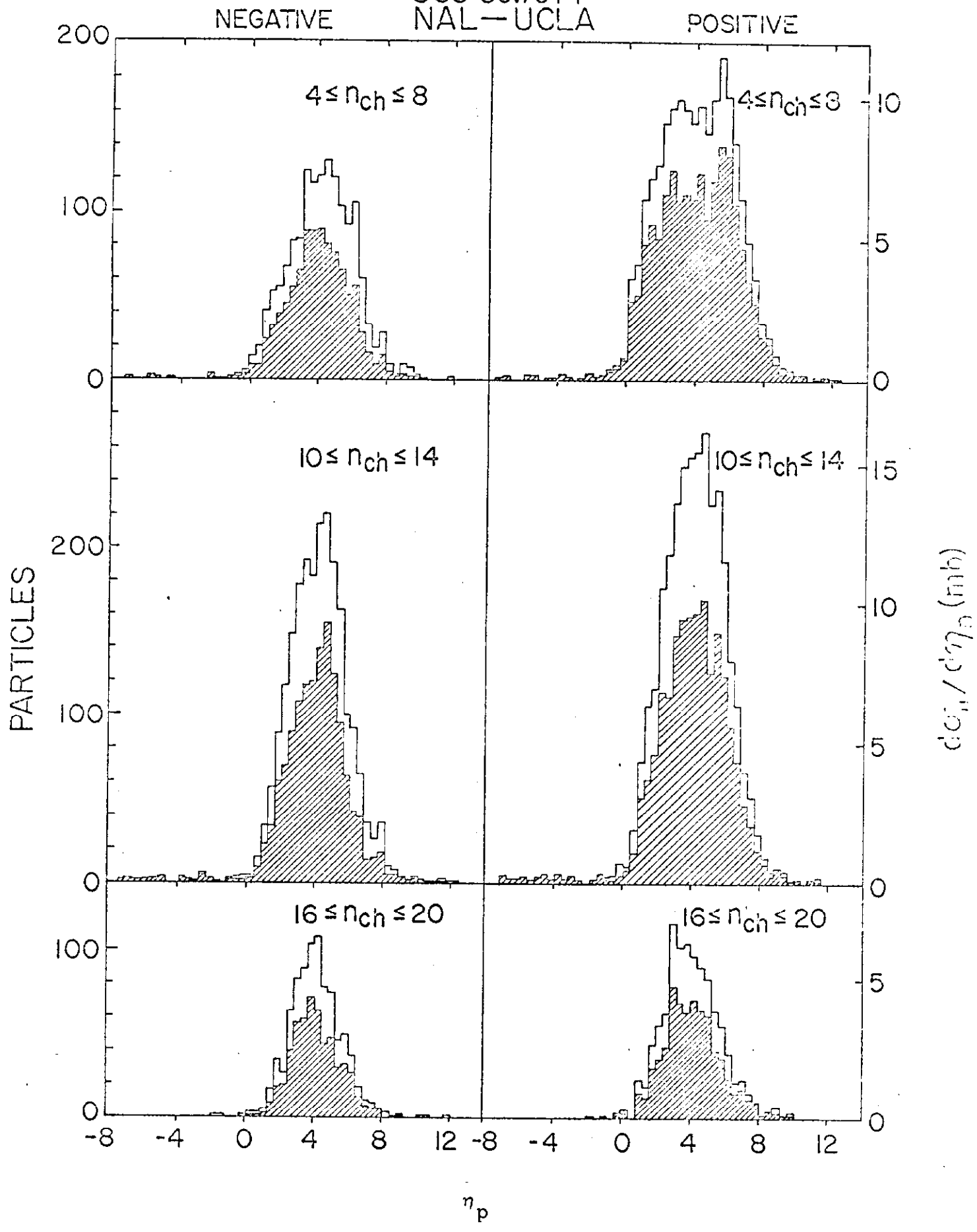


Fig. 1

NAL-UCLA 303 GeV/cPP

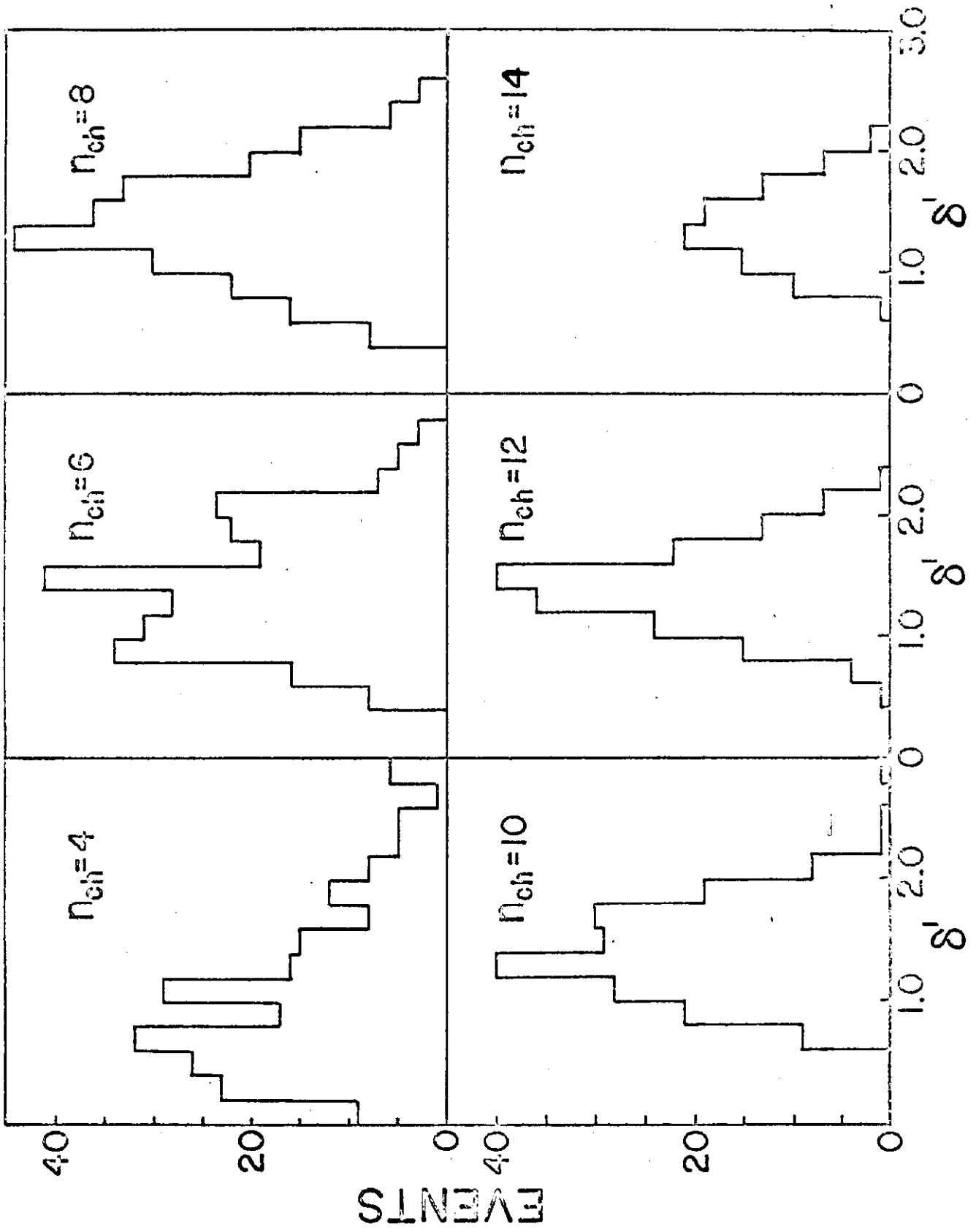


Fig. 2

